THE JOURNAL OF PHYSICAL CHEMISTRY B
A JOURNAL OF THE AMERICAN CHEMICAL SOCIETY

pubs.acs.org/JPCB Article

Effect of Branching on Mutual Solubility of Alkane–CO_2 Systems by Molecular Simulations

Kazuya Kobayashi* and Abbas Firoozabadi*

Cite This: https://doi.org/10.1021/acs.jpcb.2c05774 Read Online

ACCESS | Metrics & More | Article Recommendations | Supporting Information

ABSTRACT: Mutual solubilities of hydrocarbon–CO_2 systems are important in a broad range of applications. Experimental data and theoretical understanding of phase behavior of large hydrocarbon molecules and CO_2 are limited. This is especially true in relation to the molecular structure of hydrocarbons when the carbon number exceeds 12. In this work, the continuous fractional component Gibbs ensemble Monte Carlo simulations are used to investigate mutual solubility of different alkane and CO_2 systems and the molecular structure. We investigate the mutual solubility of *n*-decane, *n*-hexadecane, *n*-eicosane, and the corresponding structural isomers in the CO_2-rich and hydrocarbon-rich phase. The focus will be solubility of the heavy normal alkanes and their structural isomers in CO_2. The simulation results are verified by comparing the experimental data when measurements are available. The simulation of phase behavior of the *n*-decane–CO_2 system agrees with the experiments. We also present simulation results of *n*-hexadecane–CO_2 and *n*-eicosane–CO_2 systems away from the critical region partly due to the finite size effect. We establish that solubility of the hydrocarbons in CO_2 is improved by change of the molecular structure in heavier alkanes. The enhanced solubility is limited in decane isomers, but the isomers of hexadecane and eicosane show 2- to 3-time solubility enhancement. The molecular dynamics simulations suggest that the improvement is from a higher coordination number of CO_2 for methyl (CH_3) rather than for methylene (CH_2) groups. This study sets the stage for molecular engineering and synthesis of hydrocarbons that are soluble in CO_2 not only by considering functionality but also by changing the molecular structure. The solubility enhancement is the first step in viscosification of CO_2 which broadens the use of CO_2.

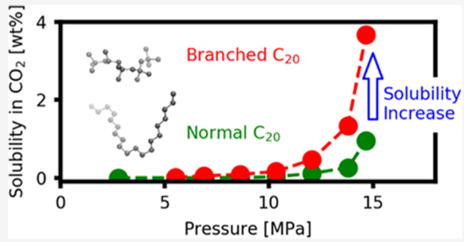

■ INTRODUCTION

Mitigation of CO_2 emission and removal of CO_2 from the atmosphere have attracted much attention because of global warming and possible disruptive effects on life on Earth. Enormous efforts are being made in capturing, storing, and utilizing CO_2 by the scientific community and industry.[1] Geological storage is widely believed to significantly reduce CO_2 emissions over other technologies (e.g., CO_2 as a feedstock).[1,2] In the geological storage, CO_2 can be stored in depleted oil and gas formations or in deep saline aquifers. Injection of CO_2 is also deployed in enhanced oil recovery (CO_2-EOR) because of higher efficiency compared to natural gas and other fluids. The efficiency of CO_2 injection in the subsurface can be drastically improved by enhancing the sweep efficiency.[3] CO_2 does not provide an efficient displacement in the subsurface because of gas-like viscosity even at high density in the supercritical state. The result is low efficiency in CO_2-EOR and the geological storage. Increase in CO_2 viscosity would lead to success in the geological storage and CO_2-EOR.

Thickeners are added to CO_2 for viscosification. This results in improvement in the mobility ratio. The degree of viscosification and solubility in CO_2 are major factors to be considered in development of direct thickeners.[3] Low adsorption to the rock is a major requirement. For decades, much effort has been made to search for polymers to viscosify CO_2.[3−5] The published thickeners may not meet the three requirements (solubility, degree of viscosification, and low adsorption) simultaneously.[3] Low solubility especially limits applications of polymers for direct thickening. Al Hinai et al.[5] have investigated the solubility of 26 polymers including poly(vinyl acetate), poly(vinyl alcohol), and poly(1-decene). They show that only four polymers [poly(1-decene) with six repeat units, poly(vinyl ethyl ether), poly(iso-butyl vinyl ether), and poly(dimethylsiloxane)] are soluble in CO_2 at a temperature of 377 K and at a pressure of 55 MPa.[5] In their study, poly(1-decene) has the highest solubility of 5 wt% at ~48 MPa and ~358 K. Out of the four polymers, the poly(1-decene) and poly(vinyl ethyl ether) viscosify carbon dioxide by about 1.2−2.8-fold and 1.2−2.1-fold, respectively, at very high pressures (>50 MPa).[5] The required concentrations to achieve the increase in viscosity stated above are 5 and 2 wt% for poly(1-decene) and poly(vinyl ethyl ether), respectively. The solubility of polymers is low in CO_2 for all but a few. Fluorinated polymers rather than the hydrocarbon framework

Received: August 11, 2022
Revised: September 20, 2022

are an option for direct thickening because of the CO_2-philicity. Fluorinated polymers may viscosify CO_2 to the desirable level.[3] However, the fluorinated polymers are expensive and have a high environmental impact.[3,7] They also become more effective at concentrations above 2 to 3 wt %. Non-fluorinated polymers such as poly(1-decene) and poly(vinyl ethyl ether) have received more attention in recent years partly due to current economic and environmental requirements. Very recently, Kar and Firoozabadi[8] suggested that increase in CO_2 solubility of poly(1-decene) can be achieved by a higher number of methyl groups. It is pointed out that squalane ($C_{30}H_{62}$) with eight methyl groups is around 8 times more soluble in supercritical CO_2 than *n*-dotriacontane ($C_{32}H_{66}$). The understanding of solubility mechanisms of hydrocarbons including polymers in CO_2 is the first important step to finding a direct thickener.

The molecular structure in hydrocarbon−CO_2 systems which is based on interactions between neighboring atoms is the key to improving the solubility of functional molecules in CO_2. Experimental and simulation studies have been conducted to draw a unified picture of the relationship between hydrocarbon solubility in CO_2 and the molecular structure. Girard et al.[9] have reviewed experimental data and presented the heuristics on the solubility of polymers in CO_2: weak polymer−polymer interaction,[7,9−11] strong polymer−CO_2 interaction,[7,10] and enhanced entropy of mixing.[7,10] Silva and Orr[6] have investigated partitioning of organic molecules between the oleic and CO_2 phases and shown that branched alkanes have higher solubility in the CO_2-rich phase than normal alkanes with the same molecular weight. Their data show that the effect becomes more pronounced in alkanes larger than *n*-dodecane.[6] The molecular structure can affect the molecular interactions and the entropy of mixing. The understanding of the relationship between hydrocarbon solubility in CO_2 and the molecular structure is limited. In heavy hydrocarbons and polymers, solubility measurement in CO_2 is a challenge. Phase behavior of CO_2 with *n*-alkanes such as *n*-decane,[12−28] *n*-hexadecane,[12,17,26,29−34] and *n*-eicosane[17,29,33−37] has been investigated over decades. However, there are limited experimental data as the molecular weight of alkanes increases. There are few reports of experiments for the structural isomers especially for dodecane and larger ones. To the best of our knowledge, experimental data for phase behavior of structural isomers of alkanes with a carbon number larger than 10 are limited to isomers of decane[24] and triacontane.[34,38−40] A complete list of references for experimental data of phase behavior between alkanes and CO_2 is presented in the Supporting Information. There is limited discussion in the literature on improvement in CO_2 solubility from change of the molecular structure.[8,41] Molecular dynamics simulations suggest that interaction between fluorinated groups and CO_2 is stronger than that of poly 1-decane and poly vinyl ethyl ether.[41] This is in line with the experimental observation that fluorinated molecules have higher solubility in CO_2 than others. Solubility mechanisms in CO_2 from the molecular structure point of view have been rarely investigated. The focus has been on the effect of different chemical species on solubility in CO_2.

Molecular simulations provide molecular-scale insights in addition to properties of interest with an appropriate interaction parameter (forcefield). The simulations can be conducted under high-temperature and high-pressure conditions.[42] Equilibrium molecular dynamics,[43−48] thermodynamic integration,[49−52] Gibbs−Duhem integration,[53−57] and Gibbs ensemble Monte Carlo (GEMC)[58−62] can be used to investigate solubility and/or solubilization behavior by molecular simulations. We select GEMC in our investigation of solubility of hydrocarbons in CO_2. GEMC implicitly reproduces a two-phase equilibrium state and provides composition of both phases without creating an interfacial system. The method can be parallelized; it is efficient.

The conventional molecular simulations may not be viable for phase behavior simulations of large molecules such as polymers and CO_2. The solubility calculation is limited to small hydrocarbons like *n*-decane,[61,62] coarse-graining models,[63] and simple systems without consideration of a specific molecule.[64] Surprisingly, there have been very few attempts using molecular simulations in phase-split calculations of a mixture of a large molecule and a small solvent molecule such as CO_2. It must be emphasized that only a few studies discuss the branching effect on solubility.[64] There have been very limited measurements of solubility of heavily branched alkanes in CO_2.

In this work, GEMC simulations are conducted to investigate the relationship between hydrocarbon solubility in CO_2 and the molecular structure. The effect of branching on the solubility in CO_2 is the focus of our investigation. Our study has two parts: (1) the GEMC results are examined by comparison with experimental data and (2) the effect of branching on solubility in CO_2. We perform continuous fractional component (CFC) GEMC[65−71] simulations for hydrocarbons including *n*-decane, *n*-hexadecane, and *n*-eicosane and their structural isomers and CO_2 systems. The CFC-GEMC is the method of choice for large molecules because of partial insertion. The technique has not been used in phase-split computations for heavy hydrocarbons and CO_2 systems in the past to the best of our knowledge.

■ SIMULATION DETAILS

The CFC method allows insertion of fractional molecules in GEMC to improve the efficiency of particle transfers. The fractional molecules have a fractional parameter (λ) between 0.0 and 1.0. The interactions of the fractional molecules with other molecules are controlled by the fractional parameter. There is no interaction between the fractional molecules and other molecules when $\lambda = 0$ and full interaction when $\lambda = 1.0$. The reduction of the interactions results in efficient transfer of molecules (i.e., insertion and deletion) in GEMC simulations. In addition to the conventional MC moves (e.g., translation, rotation), CFC-GEMC implements the lambda move, swap move of fractional molecules, and identity the exchange move. The moves attempt to change the fractional parameter, to move a fractional molecule to the other box, and to swap a fractional molecule and a full molecule, respectively. The swap move is conducted when λ is small (<0.3), and the identity exchange move is conducted when λ is large (>0.7). The λ-controlled choice can improve efficiency of sampling because the swap move and the identity exchange move are likely accepted when λ is smaller and larger, respectively. By using fractional molecules, chemical potentials of each component become equal efficiently (i.e., equilibrium state) in different phases.

There is a concern that accuracy of simulation results is affected by the introduction of fractional molecules. It is generally accepted that impurities may improve efficiency of GEMC simulations without an appreciable effect on simulation

https://doi.org/10.1021/acs.jpcb.2c05774
J. Phys. Chem. B XXXX, XXX, XXX−XXX

results. The introduction of fractional molecules does not affect simulation results.[70] Not limited to the CFC method, impurity is sometimes introduced even in the conventional GEMC simulations to enhance molecular swap move from one box to the other box.[58,59] Our simulations include a maximum of a 0.02 mole fraction of fractional molecules as impurities.

In our simulations, we use 50 to 150 organic molecules and 1000 to 1500 CO_2 molecules. The number of the molecules in the systems depends on pressure. The largest system size (150 organics and 1500 CO_2) is selected when the system is in the near-critical region; GEMC generally suffers from system size dependency.[72] The transferable potentials for phase equilibria-united atom (TraPPE-UA)[73,74] and TraPPE-small force field[75,76] are used for alkanes and CO_2, respectively. Methyl and methylene units are single pseudoatoms in the force field (i.e., united atom). Lennard-Jones potential and electrostatic interaction are incorporated for nonbonded interactions.

The force field parameters may require adjustment to reproduce vapor−liquid coexistence of alkanes and CO_2. In TraPPE force fields, the Lorentz−Berthelot (LB) mixing rule is applied to determine the nonbonded parameters. In this standard procedure, it has been reported that CO_2 solubility is overestimated in the hexane and CO_2 systems.[77] The overestimation is also confirmed at the early stage of our study. Vishnyakov et al. show that modification of the mixing rule between organics and CO_2 improves the agreement with experiments.[77] We employ modifications of the LB mixing rule as follows.

$$\varepsilon_{ij} = \zeta\sqrt{\varepsilon_{ii}\varepsilon_{jj}} \tag{1}$$

$$\sigma_{ij} = 0.5(\sigma_{ii} + \sigma_{jj}) \tag{2}$$

$$\zeta = 0.95 \tag{3}$$

where ε and σ are Lennard-Jones potential parameters and i and j represent atom type indices and ζ is the modification parameter. The ζ value is 1.0 in the standard LB mixing rule. The value of 0.95 is suggested by Vishnyakov et al.[77] This choice is reported to reproduce the phase behavior of alkanes and CO_2 up to dodecane.[77] The modification is implemented only between pseudoatoms in alkanes and atoms in CO_2. The properties of pure phases reproduced by the original force field are preserved.

Bending and torsional potentials for alkanes are calculated using the following equations

$$U_{\mathrm{Bend}}(\theta) = \frac{k_\theta}{2}(\theta - \theta_{\mathrm{eq}})^2 \tag{4}$$

$$U_{\mathrm{Torsion}}(\phi) = c_0 + c_1[1 + \cos\phi] + c_2[1 - \cos 2\phi] + c_3[1 + \cos 3\phi] \tag{5}$$

where k_θ, θ, and θ_{eq} are the harmonic constant in bonding between two neighboring species, the bending angle, and the equilibrium angle for the bending potential, respectively; ϕ is the torsional angle; and c_0 to c_3 are constants for the torsional potential. The force field parameters are summarized in the Supporting Information (Tables S2 and S3). Brick-CFCMC software[65] is used in the CFC-GEMC simulations. A cutoff length of 14 Å is applied to nonbonded interactions. Analytical tail correction[78] and Ewald summation[79] are employed for long-range Lennard-Jones potential and electrostatic potential, respectively. Initial configurations are prepared by Monte Carlo simulations of single-component phases in the *NPT* ensemble for 2×10^5 MC cycles (one MC cycle consists of the same number of trial moves as the number of molecules in a system). After the equilibration of the pure phases, more than 9×10^5 MC cycles are performed to allow the systems to reach equilibrium with molecular exchanges between the two phases. More than 5×10^6 MC cycles are required to reach the equilibrium state especially when the system is in the near-critical region. The equilibrium production runs consist of 1×10^6 MC cycles. Energy, volume, density, and composition of the systems are monitored to ensure no drift during a production run. The advantage of CFCMC over the conventional MC simulations is that it provides chemical potentials by the introduction of fractional molecules. The chemical potentials of each component in each phase are also monitored. The values are presented for all the systems in the Supporting Information (Tables S4−S13).

We perform simulations of *n*-decane, *n*-hexadecane, *n*-eicosane, and their structural isomers which are *iso*-decane (2-methylnonane), 2,2,4,6,6,8,8-heptamethylnonane, and 2,2,4,4,6,6,8,10,10-nonmethylundecane with CO_2. Molecular structures of the isomers are shown in Figure 1. Simulations of binary mixtures of *n*-decane, *n*-hexadecane, *n*-eicosane, and *iso*-decane with CO_2 are conducted at temperatures at which experimental data are available for verification. Then, we predict phase behavior of the structural isomers to investigate the branching effect. The data are provided in the Supporting Information (Tables S14−S20).

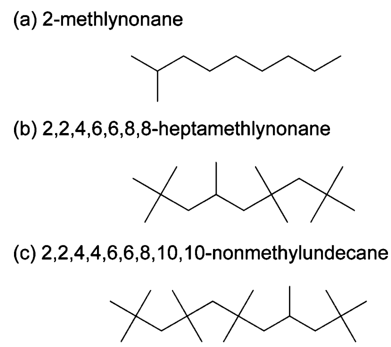

Figure 1. Molecular structure of the structural isomers of *n*-decane, *n*-hexadecane, and *n*-eicosane. (a) 2-Methylnonane, (b) 2,2,4,6,6,8,8-heptamethylnonane, and (c) 2,2,4,4,6,6,8,10,10-nonmethylundecane.

■ RESULTS AND DISCUSSION

In Figure 2, we display the pressure−composition isotherms of $nC_{10}-CO_2$; experimental data are from Reamer and Sage.[18] In the past, GEMC simulations have been performed to investigate the phase behavior with the TraPPE-UA and TraPPE-small force field.[61] The authors present the phase diagrams at a temperature of 310 K and at a pressure of 7 MPa; there is only qualitative agreement with experimental data.[61] In this work, we demonstrate that CFC-GEMC reproduces phase behavior for the *n*-decane−CO_2 system even at a higher pressure (14 MPa) and higher temperature (377.6 K) than those in ref 61. There is good agreement in the whole range. Zhang and Siepmann report overestimation of CO_2 solubility in alkanes by the TraPPE-UA forcefield which most likely is due to shortcoming of the united-atom model.[61] By modifying the LB mixing rule, the simulation results show excellent agreement with the experimental data (Figure 2). A full

https://doi.org/10.1021/acs.jpcb.2c05774
J. Phys. Chem. B XXXX, XXX, XXX−XXX

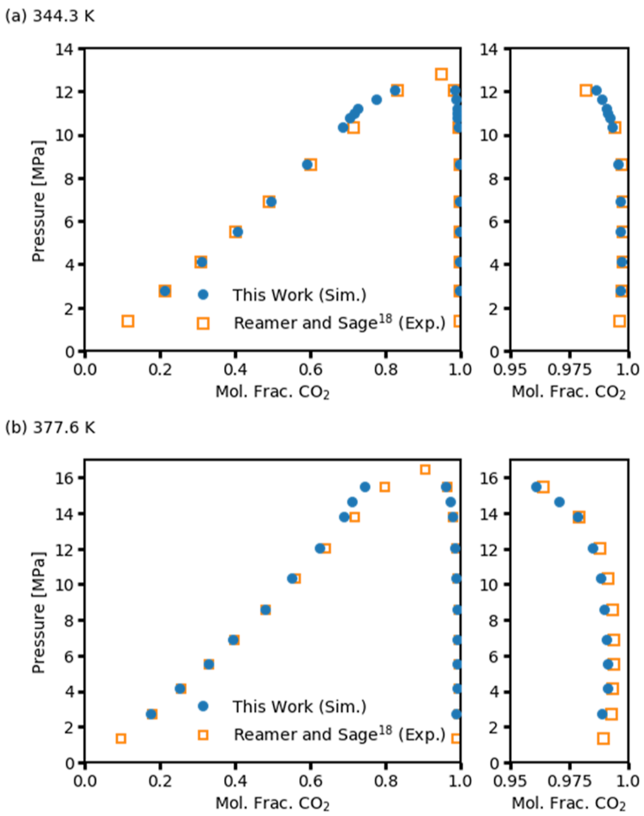

Figure 2. Pressure−composition isotherms for the *n*-decane−CO_2 system. Experimental data is from ref 18 (open squares).

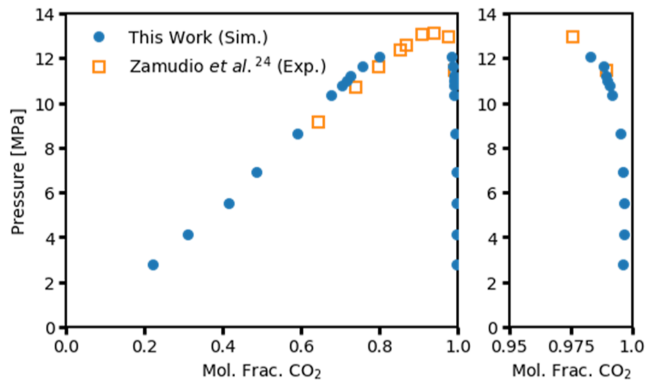

Figure 3. Pressure−composition isotherm for the *iso*-decane (2-methylnonane)−CO_2 system at 344.3 K. Experimental data is from ref 24 (open squares).

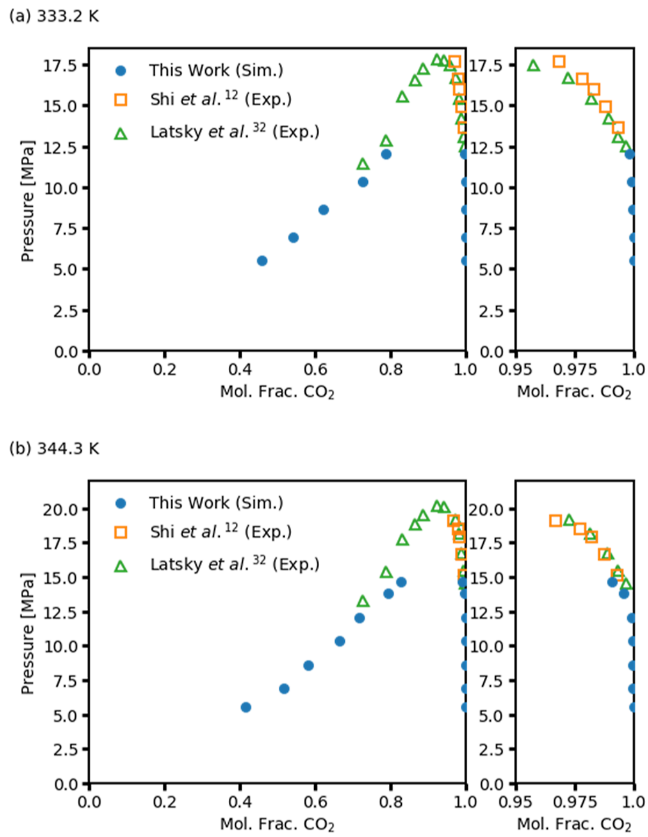

Figure 4. Pressure−composition isotherms of the *n*-hexadecane−CO_2 system. Experimental data are from ref 12 (343 K) (open squares) and ref 32 (348 K) (open triangles).

atomistic model (TraPPE-EH) may not require modifications of the mixing rule to reproduce experimental data in CO_2−alkane systems.[62] However, we recommend the use of the united atom with the mixing rule modification. The united atom reduces computational cost in simulations of phase behavior of mixtures of heavier alkanes and CO_2.

We also perform simulations of phase behavior of the structural isomer of the *n*-decane and CO_2 system. To the best of our knowledge, no studies by GEMC have been conducted for branched alkane and CO_2 systems. Recently, experimental data have been published for the *iso*-decane and CO_2 system.[24] Figure 3 shows the comparison of the phase behavior of *iso*-decane (2-methylnonane) and CO_2. Our simulations reproduce the experimental data.

Pressure−composition isotherms of heavy alkanes (i.e., *n*-hexadecane and *n*-eicosane) are shown in Figures 4 and 5. The simulation results agree with the experiments. Due to limited system size, the simulations are carried out at pressures below that of the near-critical region. In contrast to those of *n*-decane and *iso*-decane systems, the simulations become unstable at higher pressures even in the very large system size (150 alkane and 1500 CO_2 molecules).

We like to point out that experimental data are sometimes inconsistent in the heavier alkanes because of high critical pressure of the binary system (over 15 MPa), and solubility of heavier alkanes in CO_2 is extremely low. Figure 4 shows experimental data for the pressure−composition diagram in *n*-hexadecane−CO_2 systems measured at 333.2 and 343.2 K. The data are from two different groups. We like to point out that the measurements in ref 31 are significantly different from measurements in refs 12 and 32. There are challenges in high-pressure phase behavior measurements of heavy alkane−CO_2.

It is widely known both experimentally and theoretically that molecules become less soluble in CO_2 with increasing molecular weight. Flory−Huggins theory suggests that solubility will decrease with the increasing polymerization degree. However, solubility in CO_2 depends not only on molecular weight but also on the molecular structure which is not accounted for in Flory−Huggins theory. Pressure−composition isotherms for the isomers of *n*-hexadecane and *n*-eicosane are provided in the Supporting Information (Figures S1 and S2). The solubility of CO_2 in the hydrocarbon-rich phase is not appreciably affected by the molecular structure, while solubility of hydrocarbons in the

https://doi.org/10.1021/acs.jpcb.2c05774
J. Phys. Chem. B XXXX, XXX, XXX−XXX

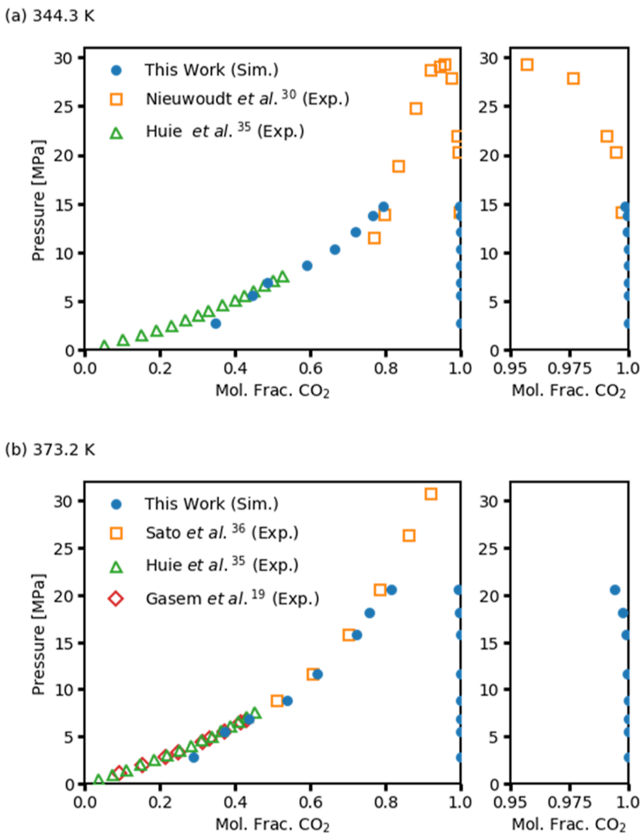

Figure 5. Pressure−composition isotherms for the *n*-eicosane−CO_2 system. Experimental data is from ref 30 (348.3 K) [open squares in (a)], ref 35 (348.2 and 373.2 K) (open triangles), ref 36 (373.2 K) [open squares in (b)], and ref 19 (373.2 K) (open diamonds).

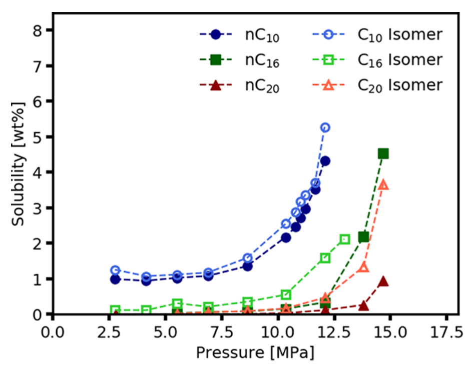

Figure 6. Solubility of alkanes in CO_2 vs pressure at 344.3 K. The results are based on CFC-GEMC simulations.

CO_2-rich phase is significantly affected as we will discuss in the following.

The solubility of normal alkanes and branched alkanes in CO_2 is presented in Figure 6. This a key plot in our work which reveals the difference in solubility of normal alkanes and branched alkanes. The plot demonstrates that branching improves the solubility in CO_2. The simulation results suggest that branching enhances solubility in CO_2 as molecular weight of an alkane increases. Decane (C_{10}) systems have no significant solubility improvement from branching (filled and open circles in Figure 6). In contrast, hexadecane and eicosane (C_{16} and C_{20}) systems clearly show solubility improvement by branching (filled and open squares for C_{16} and filled and open triangles for C_{20}). The improvements are more than 3 times. Quantitatively, 0.33 wt% of *n*-hexadecane (at T = 344.3 K) can dissolve in CO_2 at 12 MPa, while 2,2,4,6,6,8,8-heptamethylnonane has a solubility of 1.6 wt% at the same pressure. The solubility of eicosane improves from 0.95 to 3.7 wt% at 14.8 MPa (T = 344.3 K) by the molecular structure change from linear to branching with the same molecular weight. Our results are consistent with branched alkane measurements in a crude oil which shows higher solubility in a CO_2-rich phase when molecular weight of alkanes is higher than that of dodecane.[4] The data by Silva and Orr show that there is no significant difference between partitioning of iso-alkanes and normal alkanes of lower molecular weight (less than that of dodecane), whereas there is about 2- to 3-time difference in partitioning of C_{16} and C_{30}. One may reason that 2-methylnonane (structural isomer of *n*-decane) because of one branch has CO_2 solubility close to that of *n*-decane (Figure 1). To examine the effect of further branching in decane, we simulate a highly branched structural isomer of *n*-decane (2,3,4,5-tetramethylhexane). Figure S3 in the Supporting Information shows that the solubility of a highly branched decane in CO_2 does not improve from the increase in branched structures.

The largest alkane in our CFC-GEMC simulations is eicosane in the investigation into the effect of branching on CO_2 solubility. The effect of branching on CO_2 solubility increases with increase in molecular weight. Only a few studies discuss the branching effect on CO_2 solubility.[64]

We have also performed molecular dynamics simulations to compare solvation structures in normal alkanes and branched alkanes. GROMACS ver 2021.5.[80] is used for molecular dynamics simulations (simulation detail is presented in the Supporting Information). The force field used in our molecular dynamics simulations is the same as that used in the CFC-GEMC simulations. The LINCS[81] algorithm is used to fix bond length during the simulations. Each system consists of 1 organic molecule and 5000 CO_2 molecules. Figure 7 shows the radial distribution function and coordination number of carbon atoms in CO_2 around CH_3 and CH_2 groups at two different pressures. We observe that the CH_3 group has a higher number of CO_2 atoms in the first solvation shell than the CH_2 group. The implication is that branched alkanes have higher solubility in CO_2 because of a higher number of CH_3 groups than normal alkanes. A higher coordination number indicates preferable interaction with CO_2. The difference in the coordination number becomes significant at higher pressure. This is in line with the results that solubility improvement becomes more significant at higher pressure (Figure 6). The radial distribution function and coordination number of the other normal and branched alkanes also show the same trend as that shown by the plots in Figure 7. The solvation structures for the eicosane systems are presented in Figures S4 and S5 in the Supporting Information. We like to point out that the all-atom force field (CGenFF)[82] gives similar results to those of the united atom for the hexadecane systems shown in Figure 7. It seems that there is not much discussion in the literature on the effect of the molecular structure on solubility of hydrocarbons in CO_2.

■ CONCLUSIONS

CO_2−hydrocarbon interactions are investigated by an efficient molecular simulation approach through the CFC-GEMC method with a focus on solubility of alkanes and the branching

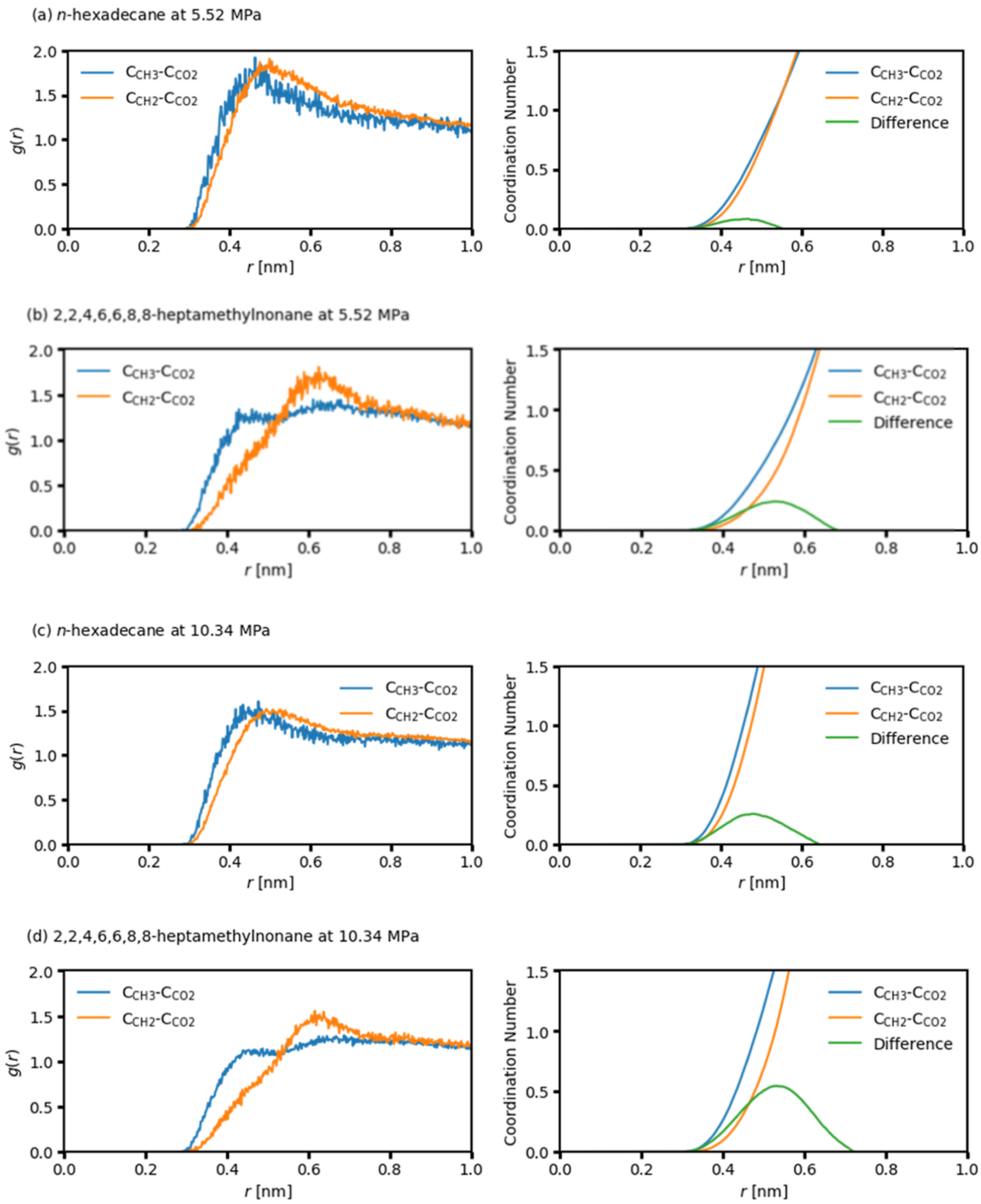

Figure 7. Solvation structure of *n*-hexadecane and its structural isomer (2,2,4,6,6,8,8-heptamethylnonane) in CO_2 at P = 5.52 and 10.34 MPa and T = 344.3 K.

effect. The interactions are of importance for application of geological storage of CO_2 and CO_2-EOR through direct thickening. Surprisingly, our current knowledge of solubility of heavy hydrocarbons in CO_2 in relation to the molecular structure is limited. We have conducted CFC-GEMC simulations to reproduce the phase behavior of CO_2 with *n*-decane, *n*-hexadecane, *n*-eicosane, and their structural isomers. It is demonstrated that the phase behavior of the *n*-decane−CO_2 system from the simulations agrees with the experiments. Molecular simulations of *n*-hexadecane−CO_2 and *n*-eicosane−CO_2 systems also show agreement with the experiments away from the critical region. Increasing the system size may allow accurate calculations at higher pressures in the critical region. One of the main objectives of the work has been extension of the calculations to structural isomers of *n*-decane, *n*-hexadecane, and *n*-eicosane to investigate molecular structure dependency of solubility in CO_2. We demonstrate that for heavier alkanes, the solubility is enhanced significantly by the molecular structure. The improvement is not pronounced in the *n*-decane isomer. The isomers of *n*-hexadecane and *n*-eicosane show 2- to 3-time improvement in solubility in CO_2. The molecular dynamics simulations suggest that the improvement is from increase in the coordination number of CO_2 for CH_3 rather than CH_2. This study proposes that the solubility improvement from branching can become significant in alkanes of higher molecular weight (e.g., polymer scale). Molecular engineering to improve the solubility in CO_2 can be achieved not only by considering functionality but also by changing the molecular structure.

■ ASSOCIATED CONTENT

Supporting Information

The Supporting Information is available free of charge at https://pubs.acs.org/doi/10.1021/acs.jpcb.2c05774.

https://doi.org/10.1021/acs.jpcb.2c05774
J. Phys. Chem. B XXXX, XXX, XXX−XXX

Reference list of experiments conducted for hydrocarbon–CO_2 systems; force field parameters used in this study; detailed simulation data; pressure–composition isotherms for isomers; solvation structure of C_{20} systems; and simulation details of molecular dynamics (PDF)

■ AUTHOR INFORMATION

Corresponding Authors

Kazuya Kobayashi – *INPEX Corporation, Tokyo 107-6332, Japan; Department of Chemical and Biomolecular Engineering, Rice University, Houston, Texas 77005, United States*; Email: kazuya.kobayashi@inpex.co.jp, kazuya.kobayashi@rice.edu

Abbas Firoozabadi – *Department of Chemical and Biomolecular Engineering, Rice University, Houston, Texas 77005, United States*; orcid.org/0000-0001-6102-9534; Email: abbas.firoozabadi@rice.edu

Complete contact information is available at: https://pubs.acs.org/10.1021/acs.jpcb.2c05774

Notes

The authors declare no competing financial interest.

■ ACKNOWLEDGMENTS

The authors would like to thank the member companies of RERI for their support.

■ REFERENCES

(1) Hepburn, C.; Adlen, E.; Beddington, J.; Carter, E. A.; Fuss, S.; Mac Dowell, N. M.; Minx, J. C.; Smith, P.; Williams, C. K. The Technological and Economic Prospects for CO_2 Utilization and Removal. *Nature* **2019**, *575*, 87–97.

(2) Mac Dowell, N.; Fennell, P. S.; Shah, N.; Maitland, G. C. The Role of CO_2 Capture and Utilization in Mitigating Climate Change. *Nat. Clim. Change* **2017**, *7*, 243–249.

(3) Enick, R. M.; Olsen, D. K.; Ammer, J. R.; Schuller, W.*Mobility and Conformance Control for CO_2 EOR via Thickeners, Foams, and Gels—A Literature Review of 40 Years of Research and Pilot Tests, SPE154122-MS*; Society of Petroleum Engineers: Richardson, TX, USA, 2012.

(4) Iezzi, A.; Enick, R.; Brady, J.Direct Viscosity Enhancement of Carbon Dioxide. *Supercritical Fluid Science and Technology*; American Chemical Society, 1989; Chapter 10, pp 122–139.

(5) Al Hinai, N. M.; Saeedi, A.; Wood, C. D.; Myers, M.; Valdez, R.; Sooud, A. K. A.; Sari, A. Experimental Evaluations of Polymeric Solubility and Thickeners for Supercritical CO_2 at High Temperatures for Enhanced Oil Recovery. *Energy Fuels* **2018**, *32*, 1600–1611.

(6) Silva, M. K.; Orr, F. M., Jr. Effect of Oil Composition on Minimum Miscibility Pressure-Part 1: Solubility of Hydrocarbons in Dense CO_2. *SPE Res. Eng.* **1987**, *2*, 468–478.

(7) Sarbu, T.; Styranec, T. J.; Beckman, E. J. Design and Synthesis of Low Cost, Sustainable CO_2-philes. *Ind. Eng. Chem. Res.* **2000**, *39*, 4678–4683.

(8) Kar, T.; Firoozabadi, A. Effective Viscosification of Supercritical Carbon Dioxide by Oligomers of 1-Decene. *iScience* **2022**, *25*, 104266.

(9) Girard, E.; Tassaing, T.; Marty, J.-D.; Destarac, M. Structure-Property Relationships in CO_2-philic (Co)polymers: Phase Behavior, Self-Assembly, and Stabilization of Water/CO_2 Emulsions. *Chem. Rev.* **2016**, *116*, 4125–4169.

(10) Rindfleisch, F.; DiNoia, T. P.; McHugh, M. A. Solubility of Polymers and Copolymers in Supercritical CO_2. *J. Phys. Chem.* **1996**, *100*, 15581–15587.

(11) Girard, E.; Tassaing, T.; Camy, S.; Condoret, J.-S.; Marty, J.-D.; Destarac, M. Enhancement of Poly(vinyl ester) Solubility in Supercritical CO_2 by Partial Fluorination: The Key Role of Polymer-Polymer Interactions. *J. Am. Chem. Soc.* **2012**, *134*, 11920–11923.

(12) Shi, Q.; Jing, L.; Qiao, W. Solubility of n-Alkanes in Supercritical CO_2 at Diverse Temperature and Pressure. *J. CO2 Util.* **2015**, *9*, 29–38.

(13) Inomata, H.; Arai, K.; Saito, S. Measurement of Vapor-Liquid Equilibria at Elevated Temperatures and Pressure Using a Flow Type Apparatus. *Fluid Phase Equilib.* **1986**, *29*, 225–232.

(14) Jiménez-Gallegos, R.; Galicia-Luna, L. A.; Elizalde-Solis, O. Experimental Vapor-Liquid Equilibria for the Carbon Dioxide + Octane and Carbon Dioxide + Decane Systems. *J. Chem. Eng. Data* **2006**, *51*, 1624–1628.

(15) Prausnitz, J. M.; Benson, P. R. Solubility of Liquids in Compressed Hydrogen, Nitrogen, and Carbon Dioxide. *AIChE J.* **1959**, *5*, 161–164.

(16) Jennings, D. W.; Schucker, R. C. Comparison of High-Pressure Vapor-Liquid Equilibria of Mixtures of CO_2 or Propane with Nonane and C_9 Alkylbenzenes. *J. Chem. Eng. Data* **1996**, *41*, 831–838.

(17) Chandler, K.; Pouillot, F. L. L.; Eckert, C. A. Phase Equilibria of Alkanes in Natural Gas Systems. 3. Alkanes in Carbon Dioxide. *J. Chem. Eng. Data* **1996**, *41*, 6–10.

(18) Reamer, H. H.; Sage, B. H. Phase Equilibrium in Hydrocarbon Systems Volumetric and Phase Behavior of the *n*-Decane-CO_2 System. *J. Chem. Eng. Data* **1963**, *2*, 468–478.

(19) Shaver, R. D.; Robinson, R. L., Jr.; Gasem, K. A. M. An Automated Apparatus for Equilibrium Phase Compositions, Densities, and Interfacial Tensions: Data for Carbon Dioxide + Decane. *Fluid Phase Equilib.* **2001**, *179*, 43–66.

(20) Nagarajan, N.; Robinson, R. L., Jr. Equilibrium Phase Compositions, Phase Densities, and Interfacial Tensions for CO_2 + Hydrocarbon Systems. 2. CO2 + *n*-Decane. *J. Chem. Eng. Data* **1986**, *31*, 168–171.

(21) Tsuji, T.; Tanaka, S.; Hiaki, T.; Saito, R. Measurements of Bubble Point Pressure for CO_2 + Decane and CO_2 + Lubricating Oil. *Fluid Phase Equilib.* **2004**, *219*, 87–92.

(22) Chou, G. F.; Forbert, R. R.; Prausnitz, J. M. High-Pressure Vapor-Liquid Equilibria for CO_2/*n*-Decane, CO_2/Tetralin, and CO_2/*n*-Decane/Tetralin at 71.1 and 104.4 °C. *J. Chem. Eng. Data* **1990**, *35*, 26–29.

(23) Iwai, Y.; Hosotani, N.; Morotomi, T.; Koga, Y.; Arai, Y. High-Pressure Vapor-Liquid Equilibria for Carbon Dioxide + Linalool. *J. Chem. Eng. Data* **1994**, *39*, 900–902.

(24) Zamudio, M.; Schwarz, C. E.; Knoetze, J. H. Phase Equilibria of Branched Isomers of C10-Alcohols and C10-Alkanes in Supercritical Carbon Dioxide. *J. Supercrit. Fluids* **2011**, *59*, 14–26.

(25) Kariznovi, M.; Nourozieh, H.; Abedi, J. Phase Composition and Saturated Liquid Properties in Binary and Ternary Systems Containing Carbon Dioxide, *n*-Decane, and *n*-Tetradecane. *J. Chem. Thermodynamics* **2013**, *57*, 189–196.

(26) Sebastian, H. M.; Simnick, J. J.; Lin, H.-M.; Chao, K.-C. Vapor-Liquid Equilibrium in Binary Mixtures of Carbon Dioxide + *n*-Decane and Carbon Dioxide + *n*-Hexadecane. *J. Chem. Eng. Data* **1980**, *25*, 138–140.

(27) Nourozieh, H.; Bayestehparvin, B.; Kariznovi, M.; Abedi, J. Equilibrium Properties of (Carbon Dioxide + *n*-Decane + *n*-Octadecane) Systems: Experiments and Thermodynamic Modeling. *J. Chem. Eng. Data* **2013**, *58*, 1236–1243.

(28) Eustaquio-Rincón, R.; Trejo, A. Solubility of *n*-Octadecane in Supercritical Carbon Dioxide at 310, 313, 333, and 353 K, in the Range 10-20 MPa. *Fluid Phase Equilib.* **2001**, *185*, 231–239.

(29) Hayduk, W.; Walter, E. B.; Simpson, P. Solubility of Propane and Carbon Dioxide in Heptane, Dodecane, and Hexadecane. *J. Chem. Eng. Data* **1972**, *17*, 59–61.

(30) Nieuwoudt, I.; du Rand, M. Measurement of Phase Equilibria of Supercritical Carbon Dioxide and Paraffins. *J. Supercrit. Fluids* **2002**, *22*, 185–199.

(31) Charoensombut-amon, T.; Martin, R. J.; Kobayashi, R. Application of a Generalized Multiproperty Apparatus to Measure

Phase Equilibrium and Vapor Phase Densities of Supercritical Carbon Dioxide in *n*-Hexadecane Systems Up to 26 MPa. *Fluid Phase Equilib.* **1986**, *31*, 89−104.

(32) Latsky, C.; Cordeiro, B.; Schwarz, C. E. High Pressure Bubble- and Dew-Point Data for Systems Containing CO_2 with 1-Decanol and *n*-Hexadecane. *Fluid Phase Equilib.* **2020**, *521*, 112702.

(33) Korkikowski, A.; Schneider, G. M. Fluid Phase Equilibria of Binary and Ternary Mixtures of Supercritical Carbon Dioxide with Low-Volatility Organic Substances Up to 100 MPa and 393 K: Cosolvency Effects and Miscibility Windows. *Fluid Phase Equilib.* **1993**, *90*, 149−162.

(34) Chai, C. P.; Paulaitis, M. E. Gas Solubilities of CO_2 in Heavy Hydrocarbons. *J. Chem. Eng. Data* **1981**, *26*, 277−279.

(35) Huie, N. C.; Luks, K. D.; Kohn, J. P. Phase-Equilibria Behavior of Systems Carbon Dioxide-*n*-Eicosane and Carbon Dioxide-*n*-Decane-*n*-Eicosane. *J. Chem. Eng. Data* **1973**, *18*, 311−313.

(36) Sato, Y.; Tagashira, Y.; Maruyama, D.; Takishima, S.; Masuoka, H. Solubility of Carbon Dioxide in Eicosane, Docosane, Tetracosane, and Octacosane at Temperatures from 323 to 473 K and Pressures Up to 40 MPa. *Fluid Phase Equilib.* **1998**, *147*, 181−193.

(37) Gasem, K. A. M.; Robinson, R. L., Jr. Solubilities of Carbon Dioxide in Heavy Normal Paraffins (C20-C44) at Pressures to 9.6 MPa and Temperatures from 323 to 423 K. *J. Chem. Eng. Data* **1985**, *30*, 53−56.

(38) Sovová, H.; Khachaturyan, J. J. M. Solubility of Squalane, Dinonyl Phthalate and Glycerol in Supercritical CO_2. *Fluid Phase Equilib.* **1997**, *137*, 185−191.

(39) Liphard, K. G.; Schneider, G. M. Phase Equilibria and Critical Phenomena in Fluid Mixtures of Carbon Dioxide + 2,6,10,15,19,23-Hexamethyltetracosane Up to 423 K and 100 MPa. *J. Chem. Thermodynamics* **1975**, *7*, 805−814.

(40) Brunner, G.; Saure, C.; Buss, D. Phase Equilibrium of Hydrogen, Carbon Dioxide, Squalene, and Squalane. *J. Chem. Eng. Data* **2009**, *54*, 1598−1609.

(41) Goicochea, A. G.; Firoozabadi, A. Atomistic and Mesoscopic Simulations of the Structure of CO_2 with Fluorinated and Non-fluorinated Copolymers. *J. Phys. Chem. C* **2019**, *123*, 17010−17018.

(42) Li, M.; Zhang, J.; Zou, Y.; Wang, F.; Chen, B.; Guan, L.; Wu, Y. Models for the Solubility Calculation of a CO_2/Polymer System: A Review. *Mater. Today Commun.* **2020**, *25*, 101277.

(43) Caddeo, C.; Mattoni, A. Atomistic Investigation of the Solubility of 3-Alkylthiophene Polymers in Tetrahydrofuran Solvent. *Macromolecules* **2013**, *46*, 8003−8008.

(44) Headen, T. F.; Boek, E. S. Molecular Dynamics Simulations of Asphaltene Aggregation in Supercritical Carbon Dioxide with and without Limonene. *Energy Fuels* **2011**, *25*, 503−508.

(45) Sun, X.; Qian, X. Atomistic Molecular Dynamics Simulations of the Lower Critical Solution Temperature Transition of Poly(*N*-vinylcaprolactam) in Aqueous Solutions. *J. Phys. Chem. B* **2019**, *123*, 4986−4995.

(46) Celia-Silva, L. G.; Vilela, P. B.; Morgado, P.; Lucas, E. F.; Martins, L. F. G.; Filipe, E. J. M. Preaggregation of Asphaltenes in the Presence of Natural Polymers by Molecular Dynamics Simulation. *Energy Fuels* **2020**, *34*, 1581−1591.

(47) Gurina, D. L.; Budkov, Y. A.; Kiselev, M. G. Impregnation of Poly(methyl methacrylate) with Carbamazepine in Supercritical Carbon Dioxide: Molecular Dynamics Simulation. *J. Phys. Chem. B* **2020**, *124*, 8410−8417.

(48) Gong, H.; Zhang, H.; Xu, L.; Li, Y.; Dong, M. Effects of Cosolvent on Dissolution Behaviors of PVAc in Supercritical CO_2: A Molecular Dynamics Study. *Chem. Eng. Sci.* **2019**, *206*, 22−30.

(49) Paluch, A. S.; Parameswaran, S.; Liu, S.; Kolavennu, A.; Mobley, D. L. Predicting the Excess Solubility of Acetanilide, Acetaminophen, Phenacetin, Benzocaine, and Caffeine in Binary Water/Ethanol Mixture Via Molecular Simulation. *J. Chem. Phys.* **2015**, *142*, 044508.

(50) Li, L.; Totton, T.; Frenkel, D. Computational Methodology for Solubility Prediction: Application to the Sparingly Soluble Solutes. *J. Chem. Phys.* **2017**, *146*, 214110.

(51) Kobayashi, K.; Liang, Y.; Sakka, T.; Matsuoka, T. Molecular Dynamics Study of Salt-Solution Interface: Solubility and Surface Charge of Salt in Water. *J. Chem. Phys.* **2014**, *140*, 144705.

(52) Aragones, J. L.; Sanz, E.; Vega, C. Solubility of NaCl in Water by Molecular Simulation Revisited. *J. Chem. Phys.* **2012**, *136*, 244508.

(53) Brennan, J.; Madden, W. G. Phase Coexistence Curves for Off-Lattice Polymer-Solvent Mixtures: Gibbs-Duhem Integration Simulations. *Mol. Sim.* **2003**, *29*, 91−100.

(54) Brennan, J.; Madden, W. G. Phase Coexistence Curves for Off-Lattice Polymer-Solvent Mixtures: Gibbs-Ensemble Simulations. *Macromolecules* **2002**, *35*, 2827−2834.

(55) van't Hof, A.; Peters, C. J.; de Leeuw, S. W. An Advanced Gibbs-Duhem Integration Method: Theory and Applications. *J. Chem. Phys.* **2006**, *124*, 054906.

(56) Lísal, M. V.; Vacek, V. Direct Evaluation of Vapour-Liquid Equilibria of Mixtures by Molecular Dynamics Using Gibbs-Duhem Integration. *Mol. Sim.* **1996**, *18*, 75−99.

(57) Kofke, D. A. Direct Evaluation of Phase Coexistence by Molecular Simulation Via Integration along the Saturation Line. *J. Chem. Phys.* **1993**, *98*, 4149−4162.

(58) Martin, M. G.; Siepmann, J. I. Predicting Multicomponent Phase Equilibria and Free Energies of Transfer for Alkanes by Molecular Simulation. *J. Am. Chem. Soc.* **1997**, *119*, 8921−8924.

(59) Wick, C. D.; Siepmann, J. I.; Theodorou, D. N. Microscopic Origins for the Favorable Solvation of Carbonate Ether Copolymers in CO_2. *J. Am. Chem. Soc.* **2006**, *127*, 12338−12342.

(60) Anderson, K. E.; Siepmann, J. I. Solubility in Supercritical Carbon Dioxide: Importance of the Poynting Correction and Entrainer Effects. *J. Phys. Chem. B* **2008**, *112*, 11374−11380.

(61) Zhang, L.; Siepmann, J. I. Pressure Dependence of the Vapor-Liquid-Liquid Phase Behavior in Ternary Mixtures Consisting of *n*-Alkanes, *n*-Perfluoroalkanes, and Carbon Dioxide. *J. Phys. Chem. B* **2005**, *109*, 2911−2919.

(62) Potoff, J. J.; Siepmann, J. I. Vapor-Liquid Equilibria of Mixtures Containing Alkanes, Carbon Dioxide, and Nitrogen. *AIChE J.* **2001**, *47*, 1676−1682.

(63) Du, Q.; Yang, Z.; Yang, N.; Yang, X. Coarse-Grained Model for Perfluorocarbons and Phase Equilibrium Simulation of Perfluorocarbons/CO_2 Mixtures. *Ind. Eng. Chem. Res.* **2010**, *49*, 8271−8278.

(64) van Vliet, R. E.; Hoefsloot, H. C. J.; Iedema, P. D. Mesoscopic Simulation of Polymer-Solvent Phase Separation: Linear Chain Behavior and Branching Effects. *Polymer* **2003**, *44*, 1757−1763.

(65) Hens, R.; Rahbari, A.; Caro-Ortiz, S.; Dawass, N.; Erdős, M.; Poursaeidesfahani, A.; Salehi, H. S.; Celebi, A. T.; Ramdin, M.; Moultos, O. A.; Dubbeldam, D.; Vlugt, T. J. H. Open Source Software for Monte Carlo Simulations of Phase and Reaction Equilibria Using the Continuous Fractional Component Method. *J. Chem. Inf. Model.* **2020**, *60*, 2678−2682.

(66) Shi, W.; Maginn, E. J. Continuous Fractional Component Monte Carlo: An Adaptive Biasing Method for Open System Atomistic Simulations. *J. Chem. Theory Comput.* **2007**, *3*, 1451−1463.

(67) Poursaeidesfahani, A.; Torres-Knoop, A.; Dubbeldam, D.; Vlugt, T. J. H. Direct Free Energy Calculation in the Continuous Fractional Component Gibbs Ensemble. *J. Chem. Theory Comput.* **2016**, *12*, 1481−1490.

(68) Rahbari, A.; Hens, R.; Nikolaidis, I. K.; Poursaeidesfahani, A.; Ramdin, M.; Economou, I. G.; Moultos, O. A.; Dubbeldam, D.; Vlugt, T. J. H. Computation of Partial Molar Properties Using Continuous Fractional Component Monte Carlo. *Mol. Phys.* **2018**, *116*, 3331−3344.

(69) Poursaeidesfahani, A.; Hens, R.; Rahbari, A.; Ramdin, M.; Dubbeldam, D.; Vlugt, T. J. H. Efficient Application of Continuous Fractional Component Monte Carlo in the Reaction Ensemble. *J. Chem. Theory Comput.* **2017**, *13*, 4452−4466.

(70) Rosch, T. W.; Maginn, E. J. Reaction Ensemble Monte Carlo Simulation of Complex Molecular Systems. *J. Chem. Theory Comput.* **2011**, *7*, 269−279.

(71) Poursaeidesfahani, A.; Rahbari, A.; Torres-Knoop, A.; Dubbeldam, D.; Vlugt, T. J. H. Computation of Thermodynamic

Properties in the Continuous Fractional Component Monte Carlo Gibbs Ensemble. *Mol. Sim.* **2017**, *43*, 189−195.

(72) Valleau, J. P. Number-Dependence Concerns in Gibbs-Ensemble Monte Carlo. *J. Chem. Phys.* **1998**, *108*, 2962.

(73) Martin, M. G.; Siepmann, J. I. Transferable Potentials for Phase Equilibria. 1. United-Atom Description of *n*-Alkanes. *J. Phys. Chem. B* **1998**, *102*, 2569−2577.

(74) Martin, M. G.; Siepmann, J. I. Novel Configurational-Bias Monte Carlo Method for Branched Molecules. Transferable Potentials for Phase Equilibria. 2. United-Atom Description of Branched Alkanes. *J. Phys. Chem. B* **1999**, *103*, 4508−4517.

(75) Potoff, J. J.; Siepmann, J. I. Vapor-Liquid Equilibria of Mixtures Containing Alkanes, Carbon Dioxide, and Nitrogen. *AIChE J.* **2004**, *47*, 1676−1682.

(76) Zhang, L.; Siepmann, J. I. Direct Calculation of Henry's Law Constants from Gibbs Ensemble Monte Carlo Simulations: Nitrogen, Oxygen, Carbon Dioxide and Methane in Ethanol. *Theor. Chem. Acc.* **2006**, *115*, 391−397.

(77) Vishnyakov, A.; Weathers, T.; Hosangadi, A.; Chiew, Y. C. Molecular Models for Phase Equilibria of Alkanes with Air Components and Combustion Products I. Alkane Mixtures with Nitrogen, CO_2, and Water. *Fluid Phase Equil* **2020**, *514*, 112553.

(78) Allen, M. P.; Tildesley, D. J.*Computer Simulation of Liquids*, 2nd ed.; Oxford University Press: Great Clarendon Street, Oxford, OX2 6DP, United Kingdom, 2017.

(79) Ewald, P. P. The Calculation of Optical, and Electrostatic Grid Potential. *Ann. Phys.* **1921**, *369*, 253.

(80) Lindahl, A.; Hess, B.; van der, S.*GROMACS 2021.5 Source code (2021.5)*; Zenodo, 2022.

(81) Hess, B.; Bekker, H.; Berendsen, H. J. C.; Fraaije, J. G. E. M. A Linear Constraint Solver for Molecular Simulations. *J. Comp. Chem.* **1997**, *18*, 1463−1472.

(82) Vanommeslaeghe, K.; Hatcher, E.; Acharya, C.; Kundu, S.; Zhong, S.; Shim, J.; Darian, E.; Guvench, O.; Lopes, P.; Vorobyov, I.; Mackerell, J. A. D. CHARMM General Force Field (CGenFF): A Force Field for Drug-Like Molecules Compatible with the CHARMM All-Atom Additive Biological Force Fields. *J. Comput. Chem.* **2010**, *31*, 671−690.

https://doi.org/10.1021/acs.jpcb.2c05774
J. Phys. Chem. B XXXX, XXX, XXX−XXX